Vibration and Dynamic Stability of Pipes Conveying Fluid on Elastic Foundations

Bong-Jo Ryu*
Department of Mechanical Design Engineering, Hanbat National University, San 16-1, Duckmyoung-dong, Yuseong-gu, Daejeon 305-764, Korea
Si-Ung Ryu, Geon-Hee Kim
Operation & Research Division, Korea Basic Science Institute, 52, Yeoeun-dong, Yuseong-gu, Daejeon 305-333, Korea
Kyung-Bin Yim
Department of Mechanical Engineering, Dongyang Technical College, 62-160, Gocheok-dong, Guro-gu, Seoul 152-714, Korea

The paper deals with the vibration and dynamic stability of cantilevered pipes conveying fluid on elastic foundations. The relationship between the eigenvalue branches and corresponding unstable modes associated with the flutter of the pipe is thoroughly investigated. Governing equations of motion are derived from the extended Hamilton's principle, and a numerical scheme using finite element methods is applied to obtain the discretized equations. The critical flow velocity and stability maps of the pipe are obtained for various elastic foundation parameters, mass ratios of the pipe, and structural damping coefficients. Especially critical mass ratios, at which the transference of the eigenvalue branches related to flutter takes place, are precisely determined. Finally, the flutter configuration of the pipe at the critical flow velocities is drawn graphically at every twelfth period to define the order of the quasi-mode of flutter configuration.

Key Words : Elastic Foundations, Pipe Conveying Fluid, Eigenvalue Branches, Flutter Configuration, Structural Damping

1. Introduction

The vibration and dynamic stability problem of slender pipe systems conveying internal fluid can be encountered in many engineering applications. Some examples of such a system are heat exchange pipes, nuclear reactor fuel elements, thin-shell structures used as heat shields in aircraft engines, and certain types of valves and other components in hydraulic machinery. The study of the dynamics of the pipe conveying fluid was initiated by Ashley et al. (1950) in an attempt to explain the vibrations observed in the Trans-Arabian oil pipeline. Benjamin (1961a, 1961b) conducted experiments of articulated pipes having two degrees-of-freedom along with the theoretical studies. He pointed out that the fluid force in pipes simply-supported at both ends is conservative, and the instability type is divergence, while the fluid force in clamped-free pipe systems is non-conservative, and the instability type is flutter. The flutter of cantilevered continuous pipes conveying fluid was investigated by Gregory et al. theoretically (1961a) and experimentally (1961b).

In parallel with the above studies, the dyna-

* Corresponding Author,
E-mail : bjryu701@hanbat.ac.kr
TEL : +82-42-821-1159; **FAX** : +82-42-821-1587
Department of Mechanical Design Engineering, Hanbat National University, San 16-1, Duckmyoung-dong, Yuseong-gu, Daejeon 305-764, Korea. (Manuscript **Received** April 22, 2004; **Revised** September 3, 2004)

mic stability of pipes conveying fluid on elastic foundations, or with additional spring supports or masses, has been also studied. Especially, the effect of an elastic foundation on the fluid-conveying pipe was investigated in several studies. Stein et al. (1970) included the effect of internal pressure in the equation of motion and introduced a Winkler elastic foundation to study the dynamic characteristics of a pipe of infinite length. They pointed out that the elastic foundation is necessary to guarantee the equilibrium of the system. However, Smith et al. (1972) concluded that the elastic foundation did not increase the flutter load of a cantilevered beam on elastic foundations subjected to a follower force. Lottati et al. (1986) investigated the effect of an elastic foundation and of dissipative forces on the stability of fluid-conveying pipes. Using Galerkin's method to calculate eigen-frequencies, they concluded that the elastic foundation stiffness have a stabilizing effect for the fluid-conveying pipes. It is well known that the Winkler elastic foundation modeled as distributed springs does not increase the critical force, but increases the critical flow velocity in the problem of pipes conveying fluid.

In addition to these studies with elastic foundations, studies on dynamic stability and vibration of pipes conveying fluid with translational spring supports or lumped masses have been conducted. Becker (1979) examined the dynamics of a pipe supported by a spring. In this case, the system behaves essentially as a cantilevered pipe for a very small spring constant, and as a clamped-pined pipe for a very large spring constant. Sugiyama and his collaborators (1985) investigated the changes of instability types of a spring-supported horizontal pipe conveying fluid. In their study, they emphasized the effect of the spring position and the spring constant on the dynamic stability of the pipe through both experiment and theory. Later, Sugiyama and his colleagues (1988) investigated the combined effect of a spring and a concentrated mass on the dynamic stability of a cantilevered horizontal pipes conveying fluid. Paidoussis (1993) gave a seminar talks related to some curiosity-driven research in fluid structure interactions and its current applications. The overview of the dynamics of pipes conveying fluid is presented in the book by Paidoussis (1998). Impollonia et al. (2000) studied the effect of elastic foundations on divergence and flutter of an articulated pipe conveying fluid. Doare et al. (2002) investigated local and global instability of fluid-conveying pipes on elastic foundations.

Most of the above studies are related to the critical flow velocity and root locus of pipes conveying fluid. Only a few studies have explained the complicated relation between the flutter mode shapes of cantilevered pipes conveying fluid and the corresponding root locus without considering any vibratory modes. Recently Lim et al. (2003) conducted the nonlinear dynamic analysis of a cantilever tube conveying fluid with system identification.

The objective of the present paper is to show the transference regions of eigenvalue curves and the corresponding unstable modes of the fluid conveying cantilevered pipes on elastic foundations. It is also shown that the transference of the eigenvalue branch does not coincide with the unstable mode as it does in ordinary dynamical systems.

In this paper, the transference of the eigenvalue branches depending on the mass ratio, the structural damping of the pipe, and the elastic foundation parameters is thoroughly explained. Also, critical mass ratios of fluid-conveying pipes with elastic foundation parameters for the transference are determined for both with and without structural damping cases.

2. Analysis and Mathematical Formulation

2.1 Mathematical model

Consider a mathematical model of a fluid conveying cantilevered pipe on elastic foundations as shown in Fig. 1.

In Fig. 1, L is the total length of the pipe, k and v are the elastic foundation stiffness per unit length and the flow velocity, respectively, x and y are the axial coordinate and the vertical coordinate, respectively.

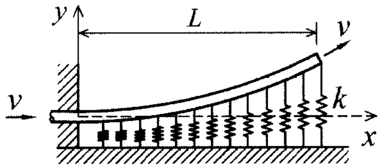

Fig. 1 Mathematical model of cantilevered pipe conveying fluid with elastic foundations

2.2 Governing equations of motion

In order to derive governing equations for a small motion of the system as shown in Fig. 1, energy expressions can be given as follows.

$$T=\int_0^L\left[\frac{m_p}{2}\left(\frac{\partial y}{\partial t}\right)^2+\frac{m_f}{2}\left\{v^2+\left(\frac{\partial y}{\partial t}+v\frac{\partial y}{\partial x}\right)^2\right\}\right]dx \quad (1)$$

$$W_c=\int_0^L\frac{m_f v^2}{2}\left(\frac{\partial y}{\partial x}\right)^2dx \quad (2)$$

$$U=\int_0^L\frac{EI}{2}\left(\frac{\partial^2 y}{\partial x^2}\right)^2dx+\frac{1}{2}\int_0^L ky^2dx \quad (3)$$

$$\delta W_{id}=-\int_0^L E^*I\left(\frac{\partial^3 y}{\partial x^2\partial t}\right)\delta\left(\frac{\partial^2 y}{\partial x^2}\right)dx \quad (4)$$

$$\delta W_{nc}=-m_f v\left[\frac{\partial y}{\partial t}+v\frac{\partial y}{\partial x}\right]_{x=l}\delta y \quad (5)$$

where, T is the total kinetic energy of the system ; W_c, the work done by the conservative component of the fluid force ; U, the elastic potential energy of the pipe ; δW_{id}, the virtual work done by internal damping ; δW_{nc}, the virtual work done by non-conservative component of the fluid force. Also, EI means the bending rigidity of the pipe. The pipe is assumed to be a viscoelastic material with the viscous resistance coefficient E^*.

In Eqs. (1) ~ (5), m_p means the pipe mass per unit length ; m_f, the fluid mass per unit length ; $y(x, t)$, the transverse displacement of the pipe at position x.

Substituting Eqs. (1) ~ (5) into the extended Hamilton's principle yields

$$\delta\int_{t_1}^{t_2}(T+W_c-U)\,dt+\int_{t_1}^{t_2}(\delta W_{id}+\delta W_{nc})\,dt=0 \quad (6)$$

Eq. (6) can be rearranged in the following form.

$$\begin{aligned}\int_{t_1}^{t_2}\int_0^L\Big[&\{m_p+m_f\}\left(\frac{\partial y}{\partial t}\right)\delta\left(\frac{\partial y}{\partial t}\right)+m_f v\left(\frac{\partial y}{\partial t}\right)\delta\left(\frac{\partial y}{\partial x}\right)\\&-E^*I\left(\frac{\partial^3 y}{\partial x^2\partial t}\right)\delta\left(\frac{\partial^2 y}{\partial x^2}\right)+m_f v\left(\frac{\partial y}{\partial x}\right)\delta\left(\frac{\partial y}{\partial t}\right)\\&+m_f v^2\left(\frac{\partial y}{\partial x}\right)\delta\left(\frac{\partial y}{\partial x}\right)-EI\left(\frac{\partial^2 y}{\partial x^2}\right)\delta\left(\frac{\partial^2 y}{\partial x^2}\right)-ky\delta y\Big]dxdt\\-\int_{t_1}^{t_2}\Big[&m_f v\left\{\left(\frac{\partial y}{\partial t}\right)+v\left(\frac{\partial y}{\partial x}\right)\right\}_{x=L}\delta y\Big]dt=0\end{aligned} \quad (7)$$

For simplicity, let us here introduce the following dimensionless parameters :

$$\xi=\frac{x}{L},\ \eta=\frac{y}{L},\ \tau=\frac{t}{L^2}\sqrt{\frac{EI}{m_f+m_p}}$$
$$K=\frac{kL^4}{EI},\ \beta=\frac{m_f}{m_f+m_p}, \quad (8)$$
$$\gamma=\frac{E^*}{EL^2}\sqrt{\frac{EI}{m_f+m_p}},\ u=vL\sqrt{\frac{m_f}{EI}}$$

where, ξ and η are the dimensionless axial and vertical coordinate, respectively. τ ; the dimensionless time, K ; the elastic foundation parameter, β ; the mass ratio, γ ; the dimensionless structural damping coefficient, and u ; the dimensionless flow velocity.

Substituting Eq. (8) into Eq. (7) leads to

$$\begin{aligned}\int_{\tau_1}^{\tau_2}\int_0^1[&\eta_\tau\delta\eta_\tau+\beta^{\frac{1}{2}}u(\eta_\tau\delta\eta_\xi+\eta_\xi\delta\eta_\tau)+u^2\eta_\xi\delta\eta_\xi\\&-\eta_{\xi\xi}\delta\eta_{\xi\xi}-\gamma\eta_{\xi\xi\tau}\delta_{\xi\xi}-K\eta\delta\eta]\,d\xi d\tau\\-\int_{\tau_1}^{\tau_2}&[\beta^{\frac{1}{2}}u\eta_\tau\delta\eta-u^2\eta_\xi\delta\eta]_{\xi=1}d\tau=0\end{aligned} \quad (9)$$

2.3 Application of finite element method

In order to obtain the numerical solutions for Eq. (9), the pipe structure is divided into N finite elements as shown in Fig. 2.

Now, introducing the following local coordinate to Eq. (9)

$$\zeta=N\xi-i+1\ (0\leq\zeta\leq1) \quad (10)$$

the following discretized equation is obtained.

$$\begin{aligned}\int_{\tau_1}^{\tau_2}\Big[&\sum_{i=1}^{N}\int_0^1\{\eta_\tau^{(i)}\delta\eta_\tau^{(i)}+\beta^{\frac{1}{2}}uN(\eta_\tau^{(i)}\delta\eta_\zeta^{(i)})+u^2N^2\eta_\zeta^{(i)}\delta\eta_\zeta^{(i)}\\&-N^4\eta_{\zeta\zeta}^{(i)}\delta\eta_{\zeta\zeta}^{(i)}-\gamma N^4\eta_{\zeta\zeta\cdot\tau}^{(i)}\delta\eta_{\zeta\zeta}^{(i)}-K\eta^{(i)}\delta\eta^{(i)}\}d\zeta\\&+\{\beta^{\frac{1}{2}}uN\eta_\tau^{(N)}\delta\eta^{(N)}+u^2N^2\eta_\zeta^{(N)}\delta\eta^{(N)}\}_{\zeta=1}\Big]d\tau=0\end{aligned} \quad (11)$$

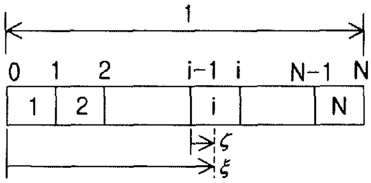

Fig. 2 Finite element model of the pipe

Now, the dimensionless displacement function $\eta(\zeta, \tau)$ can be assumed as follows:

$$\eta^{(i)}(\zeta, \tau) = \boldsymbol{f}^{(i)}(\zeta) \cdot \boldsymbol{q}^{(i)}(\tau) \tag{12}$$

where, $f(\zeta)$ means a shape function vector, and $\boldsymbol{q}(\tau)$ is a nodal displacement vector.

Substituting Eq. (12) into Eq. (11) leads to the following standard matrix form.

$$[M]\{q_{\tau\tau}\}+[C]\{q_\tau\}+[K]\{q\}=\mathbf{0} \tag{13}$$

where, $[M]$ is a global mass matrix, $[C]$ depicts a global damping matrix, and $[K]$ means a global stiffness matrix.

2.4 Stability criteria

The displacement vector $\boldsymbol{q}(\tau)$ in Eq. (13) can be assumed to be the following form.

$$\{\boldsymbol{q}(\tau)\}=\{X\}\exp(\lambda\tau) \tag{14}$$

Then, Eq. (13) can be expressed as standard eigenvalue problem.

$$\lambda[I]\{Z\}=[A]\{Z\} \tag{15}$$

where,

$$\{Z\}=\begin{Bmatrix}\{X\}\\ \{W\}\end{Bmatrix}$$
$$\{A\}=\begin{bmatrix}[0] & [I]\\ -[M]^{-1}[K] & -[M]^{-1}[C]\end{bmatrix} \tag{16}$$

In general, the system with damping has the complex characteristic roots ($\lambda_j=\sigma_j \pm j\omega_j,\ j=\sqrt{-1}$).

The stability of the system is determined by the sign of real part σ_j of the characteristic roots, λ_j.

If σ_j is negative, the system is stable. If σ_j is positive, the system is unstable. Generally speaking, there are two different unstable types (divergence and flutter) depending on the value of ω_j. However, it is noted that only the flutter type instability takes place in the present cantilevered pipe system.

If σ_j is zero, the system is critical. The configurations of stationary oscillations of the fluid-conveying pipe on elastic foundations at the critical flow velocity u_{cr} can be drawn by the following procedures.

2.5 Flutter mode shapes

If the characteristic root of the j-th branch is assumed to cross the imaginary axis at

$$\lambda_j = \pm j(\omega_j)_{cr} \tag{17}$$

where, dimensionless flow velocity u takes u_r.

Substitution of Eq. (17) into Eq. (14) gives

$$\{q(\tau)\}=\{|X_j|\}\exp(j(\omega_j)_{cr}\tau) \tag{18}$$

The critical flutter configurations for j-th eigenvector can be represented in the form.

$$\{q(\tau)\}=\{|X_j|\}\cos((\omega_j)_{cr}\tau+\phi_j) \tag{19}$$

where, the phase angle ϕ_j is given by

$$\tan\phi_j=\frac{\mathrm{Im}\{\mathbf{X}_j\}}{\mathrm{Re}\{\mathbf{X}_j\}} \tag{20}$$

3. Numerical Results and Discussion

Numerical analyses for the fluid conveying cantilevered pipe on elastic foundations were conducted by employing the finite element method.

3.1 Effect of elastic foundations and structural damping

Figures 3 and 4 show the dimensionless critical flow velocity u_{cr} for the onset of instability as a function of mass ratio β for several values of the elastic foundation parameter K, without and with structural damping, respectively. In case of no structural damping as shown in Fig. 3, the elastic foundation parameter has a stabilizing effect as noted in References (Becker, 1979; Doare et al., 2002). In Fig. 4 with structural damping, the elastic foundation parameter also increases the critical flow velocity. Therefore, one can recognize that elastic foundation parameter increases the critical flow velocity regardless of existence of structural damping, and the critical flow velocity strongly depends on the mass ratio β.

In order to investigate the effect of structural damping on the stability of fluid-conveying pipe on elastic foundations, it is necessary to represent the $(\beta,\ u)$ plane as plotted in Figs. 5 and 6. Figures 5 and show the critical flow velocity and the stable or unstable regions depending on the

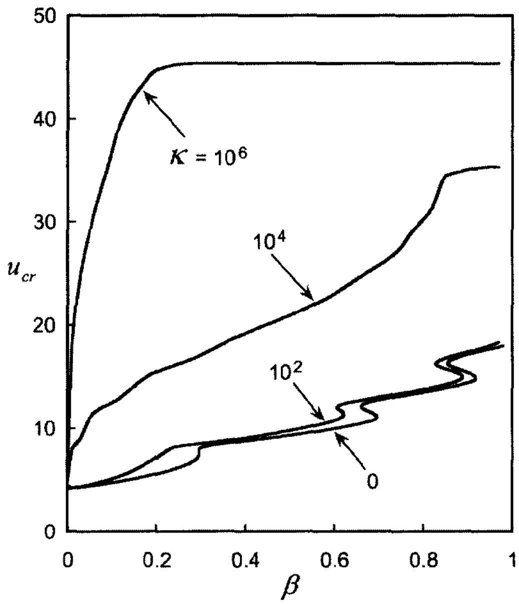

Fig. 3 Critical flow velocity depending on the mass ratio of the pipe and elastic foundation parameter (γ=0.0)

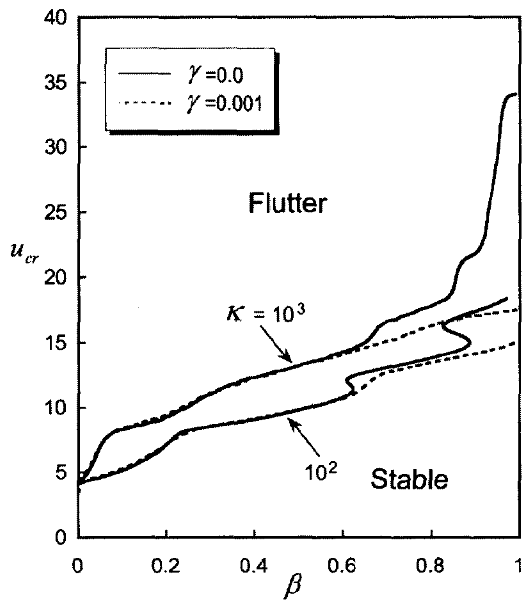

Fig. 5 Effect of internal damping on the critical flow velocity for k=100 and k=1000

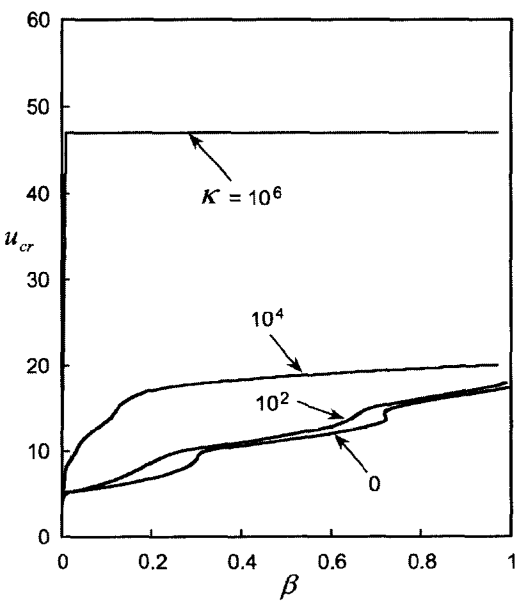

Fig. 4 Critical flow velocity depending on the mass ratio of the pipe and elastic foundation parameter (γ=0.001)

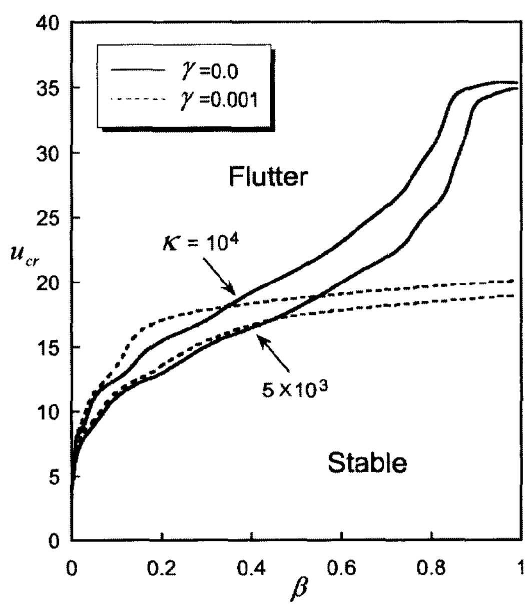

Fig. 6 Effect of internal damping on the critical flow velocity for k=5000 and k=10000

structural damping and the elastic foundation for various mass ratios β.

In Fig. 5, when $K \leq 10^3$, the destabilizing effect of the structural damping strongly appears with increasing K for a large value of the mass ratio β. In case of $K=10^2$, the structural damping decreases the critical flow velocity in the ranges of $0.63 \leq \beta < 1$, approximately. When $K=10^3$, the structural damping has a destabilizing effect for $0.6 \leq \beta < 1$.

When $K \leq 10^3$, the structural damping has, however, negligible effect on the critical flow velocity for about $\beta < 0.6$.

Figure 6 represents the (β, u) plane for $K \geq 5 \times 10^3$. In this case, the structural damping increases or decreases the critical flow velocity in front or in the rear of the special value of β.

For small values of β, in contrast to Fig. 5, the structural damping has a stabilizing effect. For large values of β, however, the structural damping decreases the critical flow velocity.

3.2 Eigenvalue branches and transference of two branches to flutter

Figure 7(a) shows the behavior of the first three eigenvalue branches for the mass ratio $\beta=0.30$ and the elastic foundation parameter $K=10^2$, with no structural damping. The horizontal axis represents the real part of eigenvalue λ, while the vertical axis represents the corresponding imaginary part. The flutter limit is determined in the root locus diagrams as the lowest flow velocity at which any branch crosses the imaginary axis.

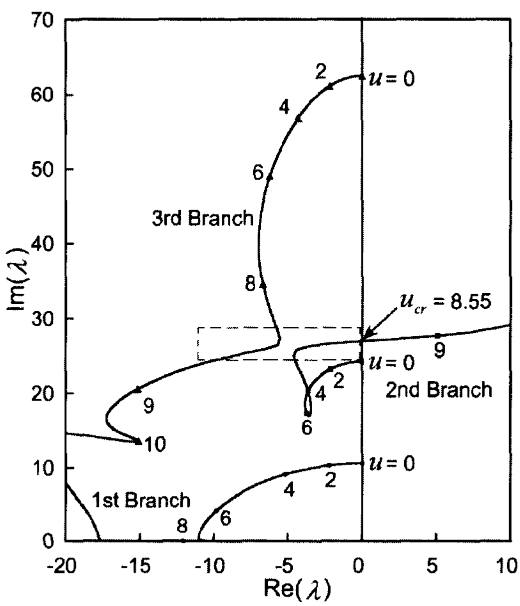

Fig. 7(a) Argand diagrams of the four lowest eigenvalues of the cantilevered pipes conveying fluid for $\beta=0.300$ ($\gamma=0.0$, $K=100$)

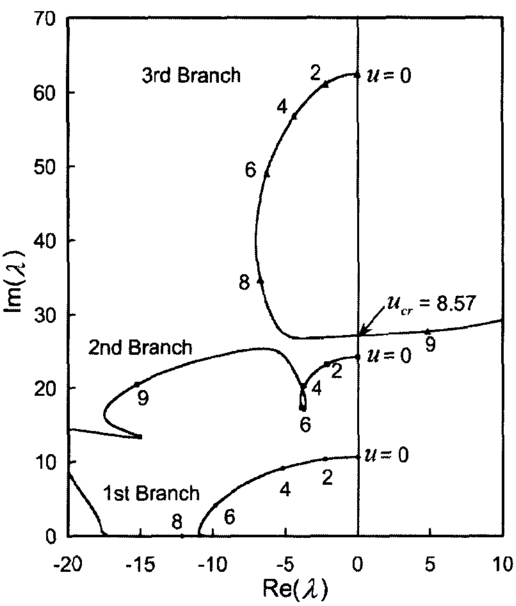

Fig. 7(b) Argand diagrams of the four lowest eigenvalues of the cantilevered pipes conveying fluid for $\beta=0.301$ ($\gamma=0.0$, $K=100$)

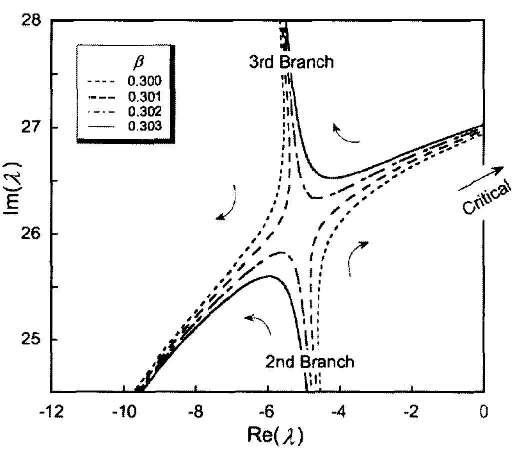

Fig. 7(c) Transfer of instability branch from the second to the third branch

As to the order of the branches, a branch that starts at the j-th natural eigen-frequency for $u=0$ is referred to here as the j-th branch (Ref. Ryu et al., 2002).

In Fig. 7(a), the flutter occurs on the second branch which starts at the second lowest frequency on the imaginary axis for the dimensionless flow velocity $u=0$.

Figure 7(b) shows the behavior of the eigenvalue branches for $\beta=0.305$. In this figure, the flutter occurs on the third branch. Figure 7(c) shows the enlarged region that is enclosed by a dotted line in Fig. 7(a). Some interesting segments of the root loci for $\beta=0.301$, 0.302 and 0.303 are added in Fig. 7(c). The second and third eigenvalue meet at a point for a mass ratio between 0.301 and 0.302. The critical mass ratio for the transference between the two branches is thus approximately $\beta_{23}=0.302$.

Figure 8(a) and 8(b) show the behavior of the eigenvalue branches for and $\beta=0.576$, in 0.580 the case with structural damping. In this case flutter occurs on the second eigenvalue branch for $\beta=0.576$, (while on the first branch for $\beta=0.580$.) Figure 8(c) shows the enlarged region enclosed by a dotted line in Fig. 8(a).

Some interesting segments of the root loci for $\beta=0.577$, 0.578 and 0.579 are added. The critical mass ratio for the transference between the two branches is approximately $\beta_{21}=0.579$.

Figures 9 and 10 show the stability map in the (β, u) plane without and with structural damping, respectively. These figures describe the rela-

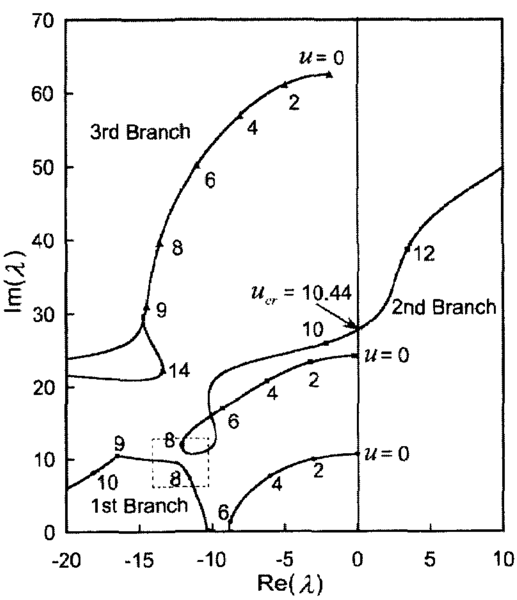

Fig. 8(a) Argand diagrams of the four lowest eigenvalues of the cantilevered pipes conveying fluid for $\beta=0.576$ ($\gamma=0.001$, $K=100$)

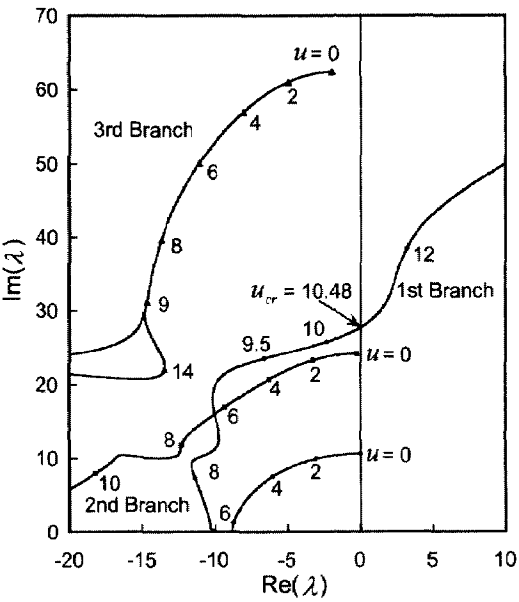

Fig. 8(b) Argand diagrams of the four lowest eigenvalues of the cantilevered pipes conveying fluid for $\beta=0.580$ ($\gamma=0.001$, $K=100$)

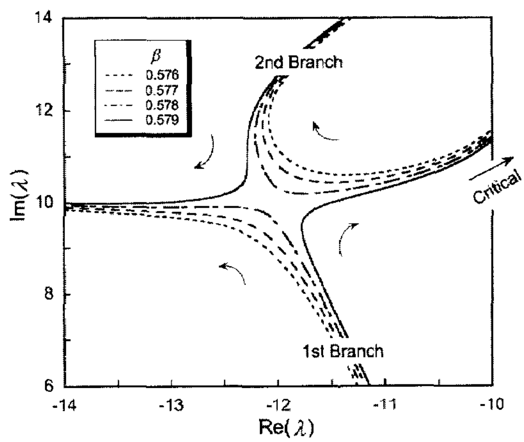

Fig. 8(c) Transfer of instability branch from the second to the first branch tion between the dimensionless critical value u_{cr} and the critical mass ratio β_{cr} associated with the transference of the two unstable branches.

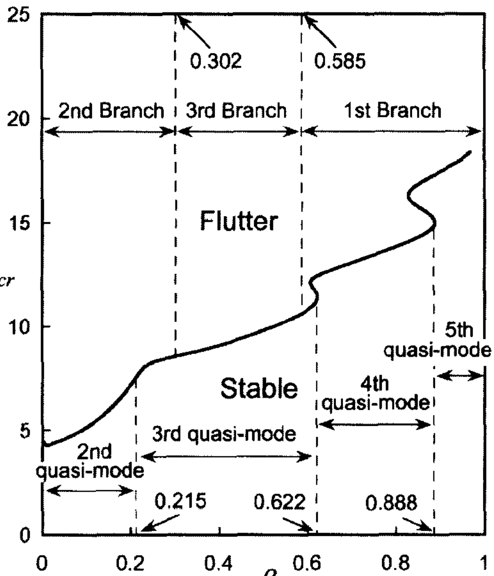

Fig. 9 Eigenvalue branches and quasi-modes depending on the mass ratio of the pipe $\gamma=0.0$, $K=100$

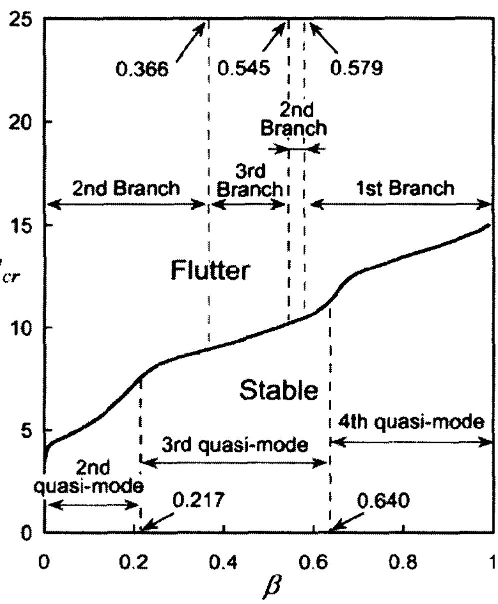

Fig. 10 Eigenvalue branches and quasi-modes depending on the mass ratio of the pipe $r=0.001$, $K=100$

In Fig. 9, the flutter occurs on the second eigenvalue branch for $0<\beta<0.302$, on the third branch for $0.302\leq\beta<0.585$, and on the first branch for $0.585\leq\beta<1.0$.

In Fig. 10, the flutter occurs on the second eigenvalue branch for $0<\beta<0.366$, on the third branch for $0.366\leq\beta<0.545$, on the second branch for $0.545\leq\beta<0.579$, and finally on the first branch for the region of $0.579\leq\beta<1.0$.

3.3 Flutter configuration

The flutter configurations in this paper can be obtained from the procedure described in section 2.4. They are drawn at every 1/12 period of the stationary oscillation. The maximum amplitude of the unstable oscillation is taken as 1/10 of the pipe length.

For the damped dynamical system of the pre-

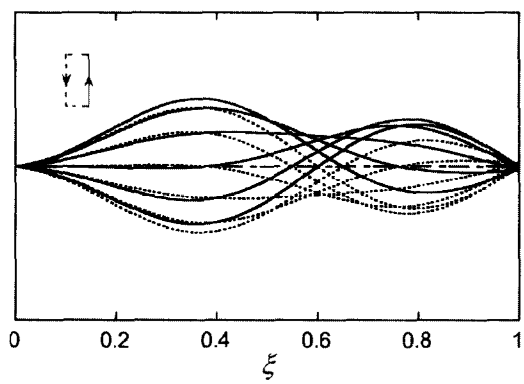

(a) $\beta=0.214$

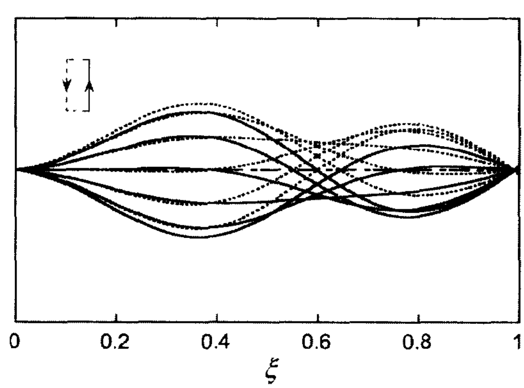

(b) $\beta=0.215$

Fig. 11 Unstable mode configurations $r=0.0$, $K=100$

sent paper, the first quasi-mode is defined as the oscillatory configuration without any moving nodes, the second with a single moving node, the third with two moving nodes, and so on (Ref. Ryu et al., 2002).

Figure 11 depict the flutter configurations without structural damping for the mass ratios $\beta=0.214$ and 0.215 when $K=100$. Figure 11(a) shows a single moving node, while Fig. 11(b) shows two moving nodes. Therefore, in Figs. 11, the flutter configuration may be referred to as the second and the third quasi-mode, respectively.

Figure 12 show the flutter configurations with structural damping for the mass ratios $\beta=0.216$ and 0.217 when $K=100$. As mentioned for Figs. 11(a) and 11(b), the flutter configurations in Figs. 12(a) and 12(b) may be referred to as the second and the third quasi-mode, respectively.

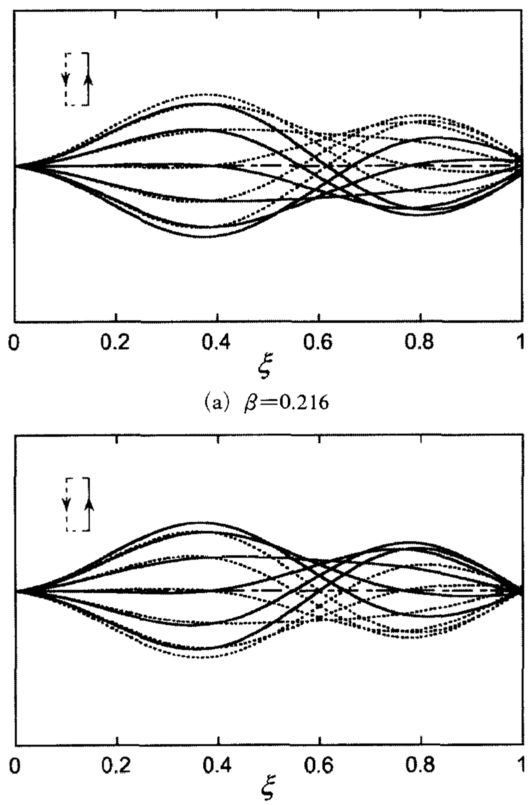

(a) $\beta=0.216$

(b) $\beta=0.217$

Fig. 12 Unstable mode configurations $\gamma=0.001$, $K=100$

4. Concluding Remarks

Through the theory and numerical simulations for the fluid conveying cantilevered pipe on elastic foundations, the following conclusions are obtained :

(1) The elastic foundation parameter K has a stabilizing effect regardless of the existence of the structural damping.

(2) For the ranges $K \leq 10^3$ and $0.6 \leq \beta < 1.0$ approximately, the structural damping has a destabilizing effect.

(3) For the range of $K > 10^3$ approximately, the structural damping has a stabilizing effect for a small value of mass ratio β, and has a destabilizing effect for a large value of mass ratio β.

Acknowledgment

This paper was supported by Academic Research Fund (2003) of Hanbat National University. The first author of this paper would like to acknowledge his appreciation for Hanbat National University.

References

Ashley, H. and Harviland, G., 1950, "Bending Vibrations of a Pipeline Containing Flowing Fluid," *Journal of Applied Mechanics, Transactions of the ASME*, Vol. 17, pp. 229~232.

Becker, O., 1979, "Zum Stabilitats verhalten des durchstromten garaden Rohres mit elasticher Querstutyung", *Maschinenbautechnik*, Vol. 28, pp. 325~327.

Benjamin, T. B., 1961, "Dynamics of a System of Articulated Pipes Conveying Fluid (I. Theory)," *Proceedings of the Royal Society (London), Series A*, Vol. 261, pp. 457~486.

Benjamin, T. B., 1961, "Dynamics of a System of Articulated Pipes Conveying Fluid (II. Experiment)," *Proceedings of the Royal Society (London), Series A*, Vol. 261, pp. 487~499.

Doare, O. and De Langre, E., 2002, "Local and Global Instability of Fluid-Conveying Pipes on

Elastic Foundations," *Journal of Fluids and Structures*, Vol. 16, No. 1, pp. 1～14.

Gregory, R. W. and Paidoussis, M. P., 1961, "Unstable Oscillation of Tubular Cantilevers Conveying Fluid (I. Theory)," *Proceedings of the Royal Society (London), Series A*, Vol. 293, pp. 512～527.

Gregory, R. W. and Paidoussis, M. P., 1961, "Unstable Oscillation of Tubular Cantilevers Conveying Fluid (II. Experiment)," *Proceedings of the Royal Society (London), Series A*, Vol. 293, pp. 528～542.

Impollonia, N. and Elishakoff, I., 2000, "Effect of Elastic Foundations on Divergence and Flutter of an Articulated Pipe Conveying Fluid," *Journal of Fluids and Structures*, Vol. 14, pp. 559～573.

Lottati, I. and Kornecki, A., 1986, "The Effect of an Elastic Foundation and of Dissipative Forces on the Stability of Fluid-conveying pipes," *Journal of Sound and Vibration*, Vol. 109, pp. 327～338.

Paidoussis, M. P., 1993, "Some Curiosity-Driven Research in Fluid Structure Interactions and Its Current Applications," *Journal of Pressure Vessel Technology, Transactions of the ASME*, Vol. 115, pp. 2～14.

Paidoussis, M. P., 1998, *Fluid-Structure Interactions : Slender Structures and Axial Flow*, Vol. 1, Academic Press.

Ryu, S. I., Sugiyama, Y. and Ryu, B. J., 2002, "Eigenvalue Branches and Modes for Flutter of Cantilevered Pipes Conveying Fluid," *Computers and Structures*, Vol. 80, pp. 1231～1241.

Smith, T. E. and Herrmann, G., 1972, "Stability of a Beam on an Elastic Foundation Subjected to a Follower Force," *Journal of Applied Mechanics, Transactions of the ASME*, Vol. 39, pp. 628～629.

Stein, R. A. and Tobriner, M. W., 1970, "Vibrations of Pipes Containing Flowing Fluids," *Journal of Applied Mechanics, Transactions of the ASME*, Vol. 19, pp. 906～916.

Sugiyama, Y., Kawagoe, H., Kishi, T. and Nishiyama, S., 1988, "Studies on the Stability of Pipes Conveying Fluid (The Combined Effect of a Spring Support and a Lumped Mass)," *JSME International Journal*, Series 1, Vol. 31, pp. 20～26.

Sugiyama, Y., Tanaka, Y., Kishi, T. and Kawagoe, H., 1985, "Effect of a Spring Support on the Stability of Pipes Conveying Fluid," *Journal of Sound and Vibration*, Vol. 100, pp. 257～270.

Lim, J. H., Jung, G. C. and Choi, Y. S., 2003, "Nonlinear Dynamic Analysis of a Cantilever Tube Conveying Fluid with System Identification," *KSME International Journal*, Vol. 17, pp. 1994～2003.